*Acta Oceanologica Sinica* 2008, Vol. 27, No. 2, p. 35 ~ 54
http://www.oceanpress.com.cn
E-mail:hyxbe@263.net

# Low-temperature alteration of oceanic island basalts and their contribution to transition metal circulation of the ocean

BU Wenrui[1*], SHI Xuefa[1], PENG Jiantang[2], LIU Jihua[1], Zhang Mingjie[3], QI Liang[2]

1. Key Laboratory of Marine Sedimentology & Environmental Geology, First Institute of Oceanography, State Oceanic Administration, Qingdao 266061, China
2. Institute of Geochemistry, Chinese Academy of Sciences, Guiyang 550002, China
3. College of Earth and Environmental Science, Lanzhou University, Lanzhou 730000, China

Received 27 February 2006; accepted 26 January 2007

## Abstract

The major elements, rare earth elements (REE) and trace elements of four basalt samples from central and western Pacific ferromanganese crust provinces have been analyzed using chemical methods and ICP – MS, respectively. The results indicate that the samples have been extensively altered and that the contents of their major elements have changed significantly. However, the similarity of REE partition patterns and trace element contents of basalt samples to those of fresh oceanic island basalts (OIB) indicate that the basalt samples originated as OIB. Because of low-temperature alteration, the contents of $Al_2O_3$, $Fe_2O_3$, MnO, $K_2O$ and $P_2O_5$ increased, while MgO and FeO decreased. Active components, such as magnesium and iron, were leached from OIB resulting in the relative enrichment of $SiO_2$. The leaching of active components can cause the relative enrichment of REE, while the precipitation of LREE-rich ferromanganese oxides in vesicles and fissures not only causes an increase of REE contents, but also induces "fractionation" of LREE and HREE. Based on the enrichment mechanism of REE contents, the theoretical quantities of precipitated ferromanganese oxides and the depleted quantities of active components are calculated: the depleted quantities of active components for the unit mass of fresh basalts vary in the range of 0.15 ~ 0.657, and the precipitated quantities of ferromanganese oxides for the unit mass of fresh basalts vary in the range of 0.006 ~ 0.042. Of the major elements, the two most depleted are iron, and magnesium, with 18.28% ~ 70.95% of iron and 44.50% ~ 93.94% of magnesium in the fresh basalts was leached out. Theoretical calculation and geochemistry results both indicate that low-temperature alteration of basalts can supply abundant amount of metals to seawater, and may play an important role in ocean metal circulation.

**Key words**: oceanic island basalts (OIB), low-temperature alteration, ocean metal circulation, theoretical calculation, cobalt-rich ferromanganese crusts

## 1 Introduction

Oceanic basalts are extruded on the ocean floor and can easily interact with seawater. For example, palagonitisation occurs gradually after the emplacement of lava flows in a submarine environment (Moore, 1966). The interaction of volcanic-seawa-

Foundation item: The National Natural Science Foundation of China (NSFC) under contract No. 40706028 and the China Oceanic Mineral Resources Research and Development Association (COMRA) under contract No. DYXM115 – 01 – 2 – 01.

* Corresponding author, E – mail: buwenrui@fio.org.cn

ter may occur in two ways (Thompson, 1991): low-temperature pervasive weathering or halmrolysis at less than 70℃, which is common and may continue for long periods of time (> 100 000 a) and high-temperature alteration, which occurs between 70 and 400℃ and is generally restricted to sites near mid-ocean ridges or intra-plate volcanoes and is relatively short lived (100 ~ 10 000 a). The low-temperature alteration of basalt is ubiquitous in the upper 500 m of oceanic crusts or more (Furnes and Staudigel, 1999; Staudigel and Hart, 1983). The primary rock texture is an important factor in determining the extent of alteration and mineral paragenesis during alteration (Pichler et al., 1999). Amorphous basalts usually have a higher rate and higher extent of alteration than crystalline basalts (Chamley, 1989).

Continued interaction of the basalts with seawater can cause variations in the mineral assemblage and chemical component of basalts. The most common products of seawater – volcanic interaction are palagonite, clay minerals (such as montmorillonite, and smectite), zeolite (phillipsite) as well as iron oxide and oxyhydroxide (Mukhopadhyay et al., 2002; Honnorez, 1981). During basalt – seawater interactions, basalts often incorporate potassium, cesium, rubidium, boron, lithium and oxygen-18 from seawater (i.e., the basalt acts as a sink, and the elements are usually incorporated into mineral phases during the alteration processes), but often lose calcium, magnesium and silicon to seawater (i.e., the basalt acts as a source) (Chester, 2000). Alteration experiments (Seyfried and Mottl, 1982) indicate that almost all magnesium, sodium, calcium, copper, zinc and carbon dioxide, and most of potassium, barium, strontium and manganese were leached out from silicate at 300℃, and aluminum, silicon and cobalt were also activated significantly. During reaction with seawater, the elements of calcium, iron, manganese, copper, zinc and silicon of basalts were leached from the basalts into seawater (Li, 1997) and then removed from seawater by oceanic sedimentation (Chamley, 1989). The alteration of basalts may play an important role in the element circulation of the ocean.

Most previous works on basalt – seawater interactions (Dang and Hou, 1995; Seewald and Seyfried, 1990; Seyfried and Mottl, 1982; Seyfried and Bischoff, 1979; Mottl and Holland, 1978) have focused on experimental studies of basalt – seawater interaction and variations of basalt composition. Pichler et al. (1999) studied the formation of secondary minerals and the behavior of elements of altered basalts from Southern Chile Ridge and Mukhopadhyay et al. (2002) compositional variations of altered basalts from the Central Indian Ocean Basin (CIOB). Here we focus attention on altered basalts from the central and western Pacific in order to study the element content variations and their geochemistry behaviors during low-temperature alteration in submarine setting, and to calculate the element content change of altered basalts theoretically, as well as to evaluate the contribution of low-temperature alteration of oceanic island basalt to ocean metal circulation.

## 2 Samples and methods

The basalt samples in this study were dredged from central and western Pacific ferromanganese crust provinces on R. V. *Dayang* No. 1 in 1999, with water depth in the range of 2 274 ~ 2 880 m (see Fig. 1).

Four samples from four dredge sites were selected for macroscopic and thin section examination. The samples were altered to various degrees, in which Sample C9 was the most altered, grey brown in color and characterized by vesicular structure. In this sample, pyroxene phenocrysts were altered to antigorites and montmorillonite, while the matrix was

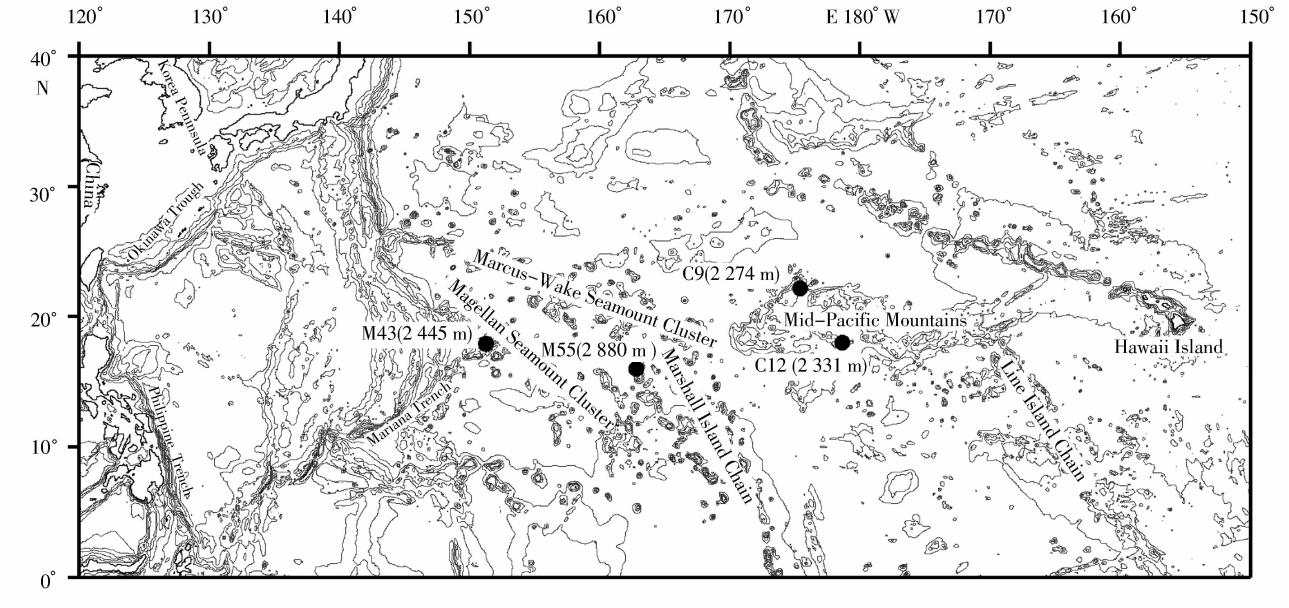


Fig. 1. Sampling location. Water depth in brackets.

altered to montmorillonite (see Fig. 2a). The sample was carbonatized with a great deal of calcite in thin section. Samples M55 and C12 are vesicular basalt with vesicle sizes about 0.5 mm on average, although some vesicles were up to 2 mm and some were filled with amygdaloids. The dominant phenocrysts in Sample M55 are augite and plagioclase, while diopside, augite and plagioclase are dominant in Sample C12. The occurrence of olivine in Samples M55 and C12 is uncertain. Sample M43 is fresher than the other samples and is dark grey, with massive structure and porphyritic texture, having dominant phenocrysts of augite and plagioclase. The presence of olivine and biotite in Sample M43 is uncertain.

In all the four samples, the matrix was devitrified with a great deal of magnetite separated out and deposited as acicular and irregular-shaped crystals, having accessory minerals of apatite, brazilite and rutile. Magnetite crystals were often separated out and deposited in the rim of dark mineral phenocrysts (see Fig. 2b). Olivine phenocrysts were usually altered into iddingsite, while inherited crystal pseudomorphism of olivine (see Fig. 2c) and some olivine phenocrysts were serpentinized. Vesicles in the basalts were often filled with zeolite (see Fig. 2d), some fissures and vesicles were filled with ferromanganese micro-nodules (see Fig. 2e) or ferromanganese oxides (see Fig. 2f).

The chemical analyses of basalt samples were carried out by the Institute of Geochemistry, Chinese Academy of Sciences. The contents of major elements were chemically analyzed, while trace elements and rare earth elements (REE) were analyzed by Finningan Mat Element high resolution ICP-MS. The analytical procedure has been described by Qi and Grégoire (2000).

## 3 Results

The contents of major elements, trace elements, REE and their diagnostic parameters are listed in Tables 1 and 2.

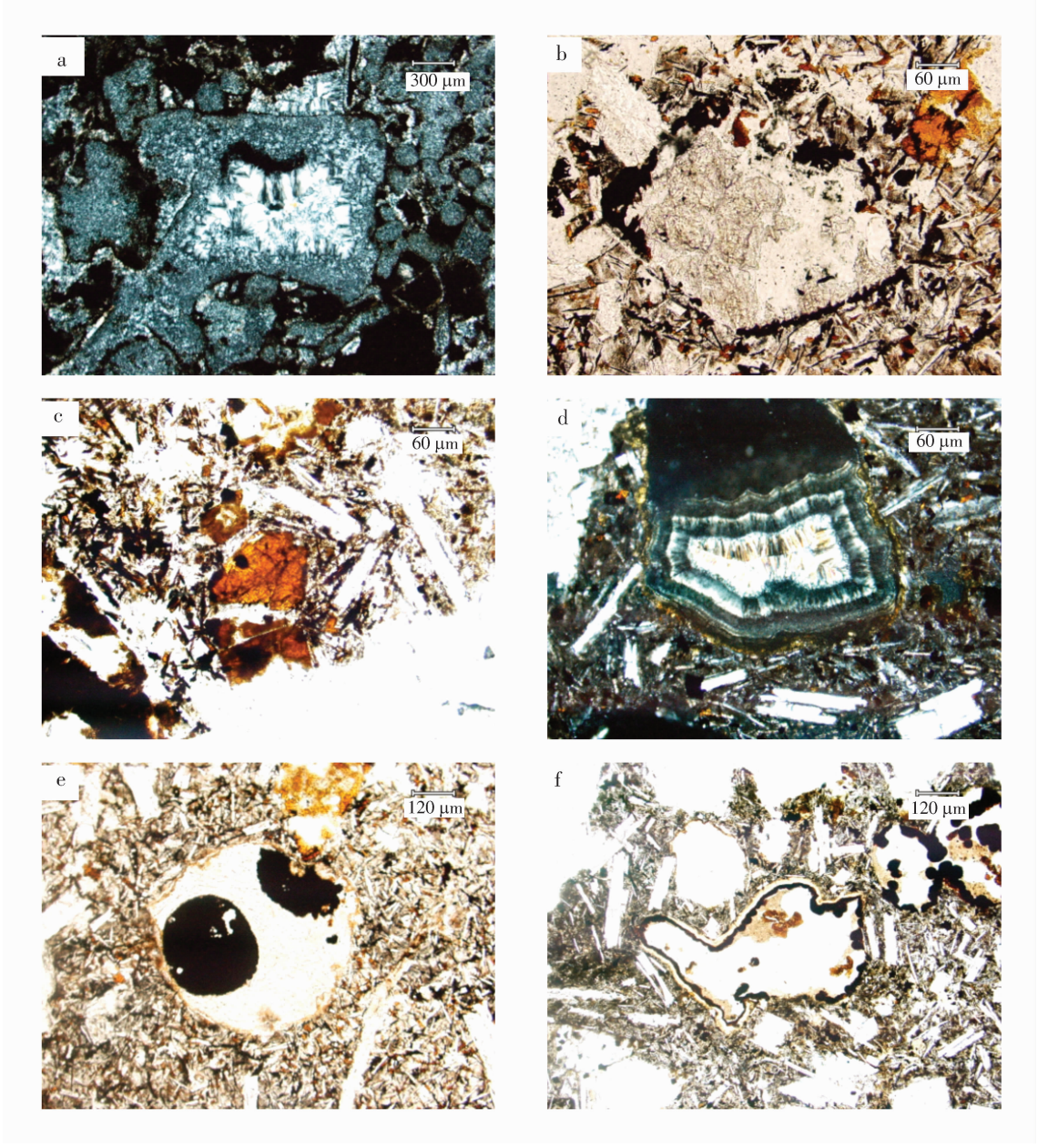


Fig. 2. Typical mineral assemblage and textural features of basalt samples. a. Remainders of pyroxene in which the central part was altered to antigorite and the marginal part altered to montmorillonite. 4 × 10( + ) (C09); b. magnetite separated from pyroxene. 20 × 10( − ) (M55); c. iddingsited olivine phenocryst. 20 × 10( − ) (C12); d. zeolite with zonal texture in vesicle of altered basalt. 20 × 10( + ) (C12); e. ferromanganese micro-nodules in vesicle of altered basalt. 10 × 10( − ) (M55); and f. ferromanganese oxides in vesicle of altered basalt. 10 × 10( − ) (C12).

Table 1. Major element contents (%), petrochemical parameters and CIPW standard mineral (after adjusted major elements contents) of altered basalt from the central and western Pacific

| | Sample No. | | | | OIB[1] | MORB | Ferromanganese crusts | | Sample No. | | | | OIB[1] | MORB |
|---|---|---|---|---|---|---|---|---|---|---|---|---|---|---|
| | C9 | C12 | M43 | M55 | | | | | C9 | C12 | M43 | M55 | | |
| | reference | | | | | | | | reference | | | | | |
| | this work | | | | Clague et al. (1980) | Schilling et al. (1983) | Hein et al. (1999) | | this work | | | | Clague et al. (1980) | Schilling et al. (1983) |
| $c(SiO_2)$[2] | 40.97 | 40.87 | 41.39 | 40.37 | 46.53 | 48.77 | 13.41 | $c(Na_2O + K_2O)$ | 5.53 | 3.85 | 2.94 | 4.36 | 3.66 | 2.51 |
| $c(TiO_2)$ | 2.37 | 2.75 | 2.17 | 2.30 | 2.25 | 1.15 | 2.22 | AR | 1.52 | 1.38 | 1.23 | 1.34 | 1.35 | 1.20 |
| $c(Al_2O_3)$ | 14.64 | 16.30 | 18.19 | 20.55 | 14.53 | 15.90 | 3.19 | $c$(Q) | 6.73 | 11.35 | 4.58 | 10.26 | 0 | 0 |
| $c(Fe_2O_3)$ | 10.25 | 11.20 | 11.63 | 10.70 | 3.15 | 1.33 | 25.43 | $c$(C) | 0.97 | 6.26 | 0.94 | 8.91 | 0 | 0 |
| $c$(FeO) | 0.55 | 0.60 | 0.87 | 0.70 | 9.51 | 8.62 | | $c$(Or) | 14.57 | 8.31 | 8.33 | 9.66 | 5.20 | 0.47 |
| $c$(MnO) | 1.42 | 0.75 | 0.26 | 0.28 | 0.19 | 0.17 | 27.11 | $c$(Ab) | 25.91 | 20.66 | 12.94 | 23.08 | 20.84 | 20.56 |
| $c$(MgO) | 1.50 | 4.70 | 5.40 | 2.20 | 9.32 | 9.67 | 2.12 | $c$(An) | 20.48 | 19.52 | 40.63 | 21.81 | 24.57 | 32.24 |
| $c$(CaO) | 11.60 | 6.20 | 9.60 | 7.50 | 10.34 | 11.16 | 3.32 | $c$(Ne) | 0 | 0 | 0 | 0 | 1.45 | 0 |
| $c(Na_2O)$ | 2.77 | 2.10 | 1.40 | 2.42 | 2.78 | 2.43 | 2.30 | $c$(Di) | 0 | 0 | 0 | 0 | 20.10 | 18.29 |
| $c(K_2O)$ | 2.23 | 1.21 | 1.29 | 1.45 | 0.88 | 0.08 | 0.78 | $c$(Hy) | 4.13 | 13.61 | 14.69 | 6.17 | 0 | 10.59 |
| $c(P_2O_5)$ | 4.33 | 0.93 | 0.63 | 1.67 | 0.29 | 0.09 | 0.98 | $c$(Ol) | 0 | 0 | 0 | 0 | 18.10 | 12.90 |
| $c$(LOI) | 4.90 | 10.35 | 6.00 | 8.06 | | | | $c$(Mt) | 0 | 0 | 0 | 0 | 4.57 | 1.93 |
| $c(CO_2)$ | 1.70 | 1.25 | 1.00 | 1.10 | | | | $c$(Il) | 4.64 | 3.34 | 2.61 | 2.34 | 4.27 | 2.18 |
| $c(Fe_2O_3)/c$(FeO) | 18.64 | 18.67 | 13.37 | 15.29 | 0.33 | 0.15 | | $c$(Hm) | 11.33 | 13.02 | 12.70 | 12.06 | 0 | 0 |
| $c$(Fe) | 8.40 | 9.66 | 9.63 | 9.05 | 9.60 | 7.64 | | $c$(Ru) | 0.18 | 1.44 | 0.99 | 1.36 | 0 | 0 |
| $\sigma$ | 13.35 | 3.28 | 3.91 | 7.63 | 3.79 | 1.09 | | $c$(Ap) | 10.45 | 2.36 | 1.50 | 4.11 | 0.63 | 0.20 |

Notes: 1) Average of 28 samples; 2) $c$ represents the content.

### 3.1 Major elements

Because of submarine alteration, the basalt samples have high LOI and carbon dioxide contents (4.90% ~ 10.4% and 1.00% ~ 1.70%, respectively) (Table 1), and a great deal of calcite was observed in basalt samples in thin section. In order to calculate the petrochemical parameters and CIPW standard mineral assemblage (Table 1), we discounted all the LOI and carbon dioxide, and a part of CaO in the ratios of calcite ($CaCO_3$) and converted the other oxides into 100%.

The four basalt samples have low $SiO_2$ contents of 40.37% ~ 41.39%, lower than the lower limit (43%) of fresh basalt. Comparing with oceanic island basalt (OIB) (Clague et al., 1980) and mid-ocean ridge basalt (MORB) (Schilling et al., 1983), the samples are significantly enriched in $Al_2O_3$, $Fe_2O_3$, MnO, $K_2O$ and $P_2O_5$, with the averages of 17.4%, 11.0%, 0.68%, 1.55% and 1.89%, respectively, but are depleted MgO and FeO with contents in the range of 1.50% ~ 5.40%

and 0.55% ~ 0.87%, respectively (see Table 1, Fig. 3), especially MgO which is very much lower than those of oceanic crusts (7.7%) (Taylor and Mclennan, 1985). The precipitation of ferromanganese oxides in altered basalts accounts for their high MnO contents (Mukhopadhyay et al., 2002).

Table 2. Rare earth elements contents (μg/g), their diagnostic parameters and trace elements contents (μg/g) of altered basalt from central and western Pacific

| | Sample No. | | | | OIB | Crust | | Sample No. | | | | OIB | Crust |
|---|---|---|---|---|---|---|---|---|---|---|---|---|---|
| | C9 | C12 | M43 | M55 | | | | C9 | C12 | M43 | M55 | | |
| | reference | | | | | | | reference | | | | | |
| | this work | | | | Hofmann et al. (1996)[1] | Hein et al. (1999) | | this work | | | | Clague et al. (1980)[2] | Hein et al. (1999) |
| *c*(La) | 161.01 | 60.57 | 83.27 | 58.64 | 20.07 | 361 | *c*(Sc) | 20.42 | 20.81 | 26.57 | 20.45 | 33.39 | 5 |
| *c*(Ce) | 131.38 | 118.23 | 134.13 | 67.31 | 50.16 | 2354 | *c*(V) | 241.29 | 178.45 | 224.24 | 207.03 | 330.36 | 626 |
| *c*(Pr) | 23.21 | 13.55 | 14.77 | 11.01 | 7.00 | 87.1 | *c*(Cr) | 251.26 | 83.37 | 475.51 | 29.53 | 552.32 | 118 |
| *c*(Nd) | 98.02 | 56.07 | 52.02 | 47.21 | 30.87 | 371 | *c*(Co) | 219.84 | 207.41 | 76.04 | 78.94 | 63.54 | 6904 |
| *c*(Sm) | 17.89 | 12.00 | 9.50 | 9.83 | 7.85 | 74.4 | *c*(Ni) | 460.88 | 238.54 | 124.38 | 88.44 | 244.46 | 3651 |
| *c*(Eu) | 4.77 | 3.26 | 2.62 | 2.73 | 2.39 | 18.3 | *c*(Cu) | 395.64 | 134.58 | 127.77 | 223.02 | 96.36 | 760 |
| *c*(Gd) | 19.84 | 10.40 | 8.66 | 10.17 | 7.25 | 69.2 | *c*(Zn) | 190.62 | 213.58 | 189.15 | 162.56 | 88.18 | 531 |
| *c*(Tb) | 2.79 | 1.47 | 1.16 | 1.52 | 1.05 | 12.7 | *c*(Rb) | 29.42 | 32.01 | 38.46 | 35.13 | 33.39 | 1715 |
| *c*(Dy) | 16.26 | 8.26 | 6.51 | 9.28 | 6.29 | 62.4 | *c*(Sr) | 1000.37 | 833.65 | 549.07 | 647.80 | 433.04 | 864 |
| *c*(Ho) | 3.34 | 1.54 | 1.21 | 1.78 | 1.20 | 11.4 | *c*(Y) | 169.25 | 45.58 | 40.10 | 66.17 | 19.96 | 178 |
| *c*(Er) | 9.52 | 4.19 | 3.38 | 4.84 | 3.05 | 30.1 | *c*(Zr) | 306.95 | 308.01 | 263.45 | 201.95 | 143.14 | |
| *c*(Tm) | 1.25 | 0.52 | 0.44 | 0.67 | 0.42 | 4.0 | *c*(Nb) | 48.59 | 81.40 | 75.04 | 49.15 | 30.87 | |
| *c*(Yb) | 6.82 | 3.36 | 2.79 | 3.93 | 2.36 | 26.0 | *c*(Ba) | 1082.08 | 585.90 | 2292.66 | 373.31 | 305.36 | 1889 |
| *c*(Lu) | 1.08 | 0.48 | 0.43 | 0.58 | 0.34 | 3.57 | *c*(Hf) | 7.71 | 7.73 | 6.95 | 4.92 | | |
| Σ*c*(REE) | 497.17 | 293.88 | 320.89 | 229.49 | 140.30 | 3485.17 | *c*(Ta) | 2.56 | 4.57 | 4.38 | 2.89 | | |
| δCe[3] | 0.45 | 0.94 | 0.84 | 0.59 | 0.99 | 3.04 | *c*(Th) | 4.15 | 6.12 | 17.79 | 4.09 | | |
| δEu[3] | 0.78 | 0.88 | 0.87 | 0.84 | 0.96 | 0.77 | *c*(Rb)/ | 0d.029 | 0.038 | 0.070 | 0.054 | 0.077 | 0.504 |
| Σ$a_t$(Ce)/ | 7.2 | 8.7 | 12.0 | 6.0 | 5.4 | 14.9 | *c*(Sr) | | | | | | |
| Σ$a_t$(Yb) | | | | | | | *c*(Zr)/ | 6.32 | 3.78 | 3.51 | 4.11 | | |
| [*c*(La)/ | 5.67 | 3.18 | 5.52 | 3.76 | 1.56 | 3.05 | *c*(Nb) | | | | | | |
| *c*(Sm)]$_{N3}$ | | | | | | | | | | | | | |

Notes: 1) average of seven samples; 2) average of 28 samples; 3) chondrite-normalized, normalization constants of chondrite after Tayor and Mclennan (1985).

The ratios of $c(Fe_2O_3)/c(FeO)$ and the contents of $H_2O$ are geochemical parameters which describe the degree of alteration of submarine basalts. Hart (1970) quantified low-temperature alteration into four stages, according to their ratios of $c(Fe_2O_3)/c(FeO)$ and $H_2O$ contents. The ratios of $c(Fe_2O_3)/c(FeO)$, and $H_2O$ and $K_2O$ contents increased with intensified alteration of the basalts,

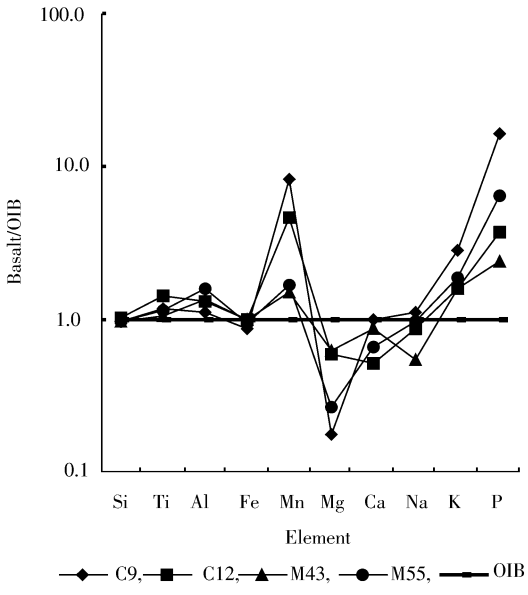


Fig. 3. OIB-normalized major element variation diagram of basalts. The major elements were adjusted for LOI and carbonate. OIB data after Clague et al. (1980) (average of 28 samples).

while MgO contents decreased (Hekinian, 1971). Fresh oceanic basalts have ratios of $c(Fe_2O_3)/c(FeO)$, and $H_2O$ contents in the ranges of 0.1 ~ 0.3 and 0.6% ~ 1.1%, and generally less than 0.2 and 1%, respectively (Miyashiro et al., 1969). Alteration of the basalts increases their $Fe^{3+}$ contents and decreases their $Fe^{2+}$ contents (Hein and Morgan, 1999) resulting in an increase in the ratios of $c(Fe_2O_3)/c(FeO)$. The basalt samples have higher contents of $Fe_2O_3$ (in the range of 10.25% ~ 11.63%) and lower contents of FeO (in the range of 0.55% ~ 0.87%) than those fresh OIB (the contents of $Fe_2O_3$ and FeO are 3.15% and 9.51%, respectively on the average) and MORB (the contents of $Fe_2O_3$ and FeO are 1.33% and 8.62%, respectively on the average). They have ratios of $c(Fe_2O_3)/c(FeO)$ of 40 ~ 125 times higher than those of OIB and MORB (see Table 1), and display characteristics of intensively altered basalts. The alteration of basalt also results in their high LOI contents (4.90% ~ 10.4%).

CIPW standard mineral contents of basalt samples are significantly different from those of OIB and MORB (see Table 1). The basalt samples are relatively enriched in $SiO_2$ and $Al_2O_3$, having the appearance of standard mineral quartz (Q) and corundum (C), with their contents in the range of 4.58% ~ 11.35% and 0.94% ~ 8.91%, respectively, and averages of 8.23% and 4.27%. Compared with OIB, the samples have no standard mineral olivine (Ol) [$2(Mg, Fe)O \cdot SiO_2$], but have standard mineral hypersthene (Hy) [$(Mg, Fe)O \cdot SiO_2$] indicating that the samples are relatively enriched in silicon and saturated with $SiO_2$; while the absence of standard mineral diopside (Di) [$CaO \cdot (Mg, Fe)O \cdot SiO_2$] is the result of depleting of CaO (the contents of CaO in silicate facies are depleted with the range of 4.67% ~ 9.63%, and other CaO occur as $CaCO_3$ in calcite with the range of 1.28% ~ 2.21%) (Qiu, 1985). The high contents of standard mineral hematite (Hm) (in the range of 11.33% ~ 13.02%) of samples correspond to their high ratios of $c(Fe_2O_3)/c(FeO)$, implying the oxidation of basalts. The samples have higher contents of standard mineral apatite (Ap) than OIB and MORB (see Table 1). This is consistent with their higher $P_2O_5$ contents compared with those of OIB and MORB as a result of phosphatization of the basalt.

The Rittmann Index ($\sigma$) of basalt samples is in the range of 3.28 ~ 13.35, with alkalinity ratios (AR) of 1.23 ~ 1.52 and bulk alkali contents [$c(Na_2O + K_2O)$] of 2.94% ~ 5.53% (see Table 1). In a TAS plot, the basalt samples plot in the basanites and tephrites areas (Le Maitre, 1989) reflecting their alkali series.

### 3.2 REE geochemistry

The samples have high and variable contents of REE, with the sum of REE content [$\Sigma c(REE)$] ranging from 229 μg/g to 497 μg/g with an average of 335 μg/g (see Table 2). The variation of

$\Sigma c$(REE) values of the samples indicates their different degrees of alteration. The higher $\Sigma c$(REE) values are therefore a consequence of the more intensive alteration of the basalts (Kang et al., 1998). The samples relatively enriched in LREE, with the $\Sigma a_t$(Ce)/$\Sigma a_t$(Yb) ratios ranging from 6.00 to 12.1 and with right inclining chondrite-normalized patterns (Fig. 4). All basalt samples have δEu and δCe values in the range of 0.78 ~ 0.88 and 0.45 ~ 0.94, respectively, suggesting a negative europium anomaly and a moderate to negative cerium anomaly. The negative europium anomaly may be a consequence of the fractionation of plagioclase from the initial magma (Wang et al., 1989), while the negative cerium anomaly may result from leaching of cerium from basalts during interaction with seawater (Chen, 1990).

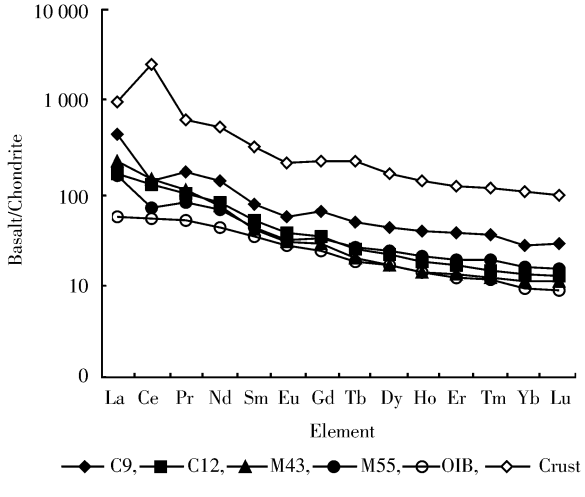


Fig. 4. Schematic chondrite-normalized REE patterns for basalt rocks. Normalization constants of chondrite after Tayor and Mclennan (1985), OIB data after Hofmann and Jochum (1996). Crust data after Hein et al. (1999) and references there in (average of 182 samples).

### 3.3 Trace element characteristics

The REE and trace element characteristics of the basalt samples are more similar to OIB than those of MORB. In primary mantle-normalized (see Fig. 5a) and MORB-normalized (see Fig. 5b) trace element spiderdiagram patterns, the patterns of the basalt samples are similar to those of OIB (Sun, 1980) and differ from those of MORB (Saunders and Tarney, 1984), suggesting that the basalt samples are petrogenetically intra plate OIB. The contents of high field strength elements (HFSE), such as tantalum, niobium, hafnium, zirconium and titanium, are higher than those of OIB (see Figs 5a and b), implying that the HFSE were relatively enriched due to their stability and the leaching of active components from basalts. The contents of barium, thorium, lanthanun, phosphorus and yttrium are relatively enriched and more variable than those of OIB (see Figs 5a and b), suggesting that these elements were enriched during low-temperature alteration or that the enrichment of the elements is related to phosphatization.

Chromium and nickel in igneous rocks are compatible elements with respect to dark minerals, such as olivine, garnet, pyroxene, hornblende, magnetite and spinel (Wilson, 1989). In chondrite-normalized transition element spiderdiagram patterns (see Fig. 6), chromium, and nickel are located in a trough, suggesting that these elements were leached out from dark minerals, which act as host for chromium and nickel were decomposed due to alteration. The systematic dispersion of chromium, nickel, manganese, cobalt and copper in chondrite-normalized spiderdiagram patterns (see Fig. 6) suggests that the contents of these elements have been changed. During long-term interaction with seawater, the contents of active elements in basalt were variable. At high temperatures, transition elements of manganese, zinc and copper are especially active (Seewald and Seyfried, 1990).

## 4 Discussion

### 4.1 Tectonic setting of basalt

The activation of trace elements and REE of ba-

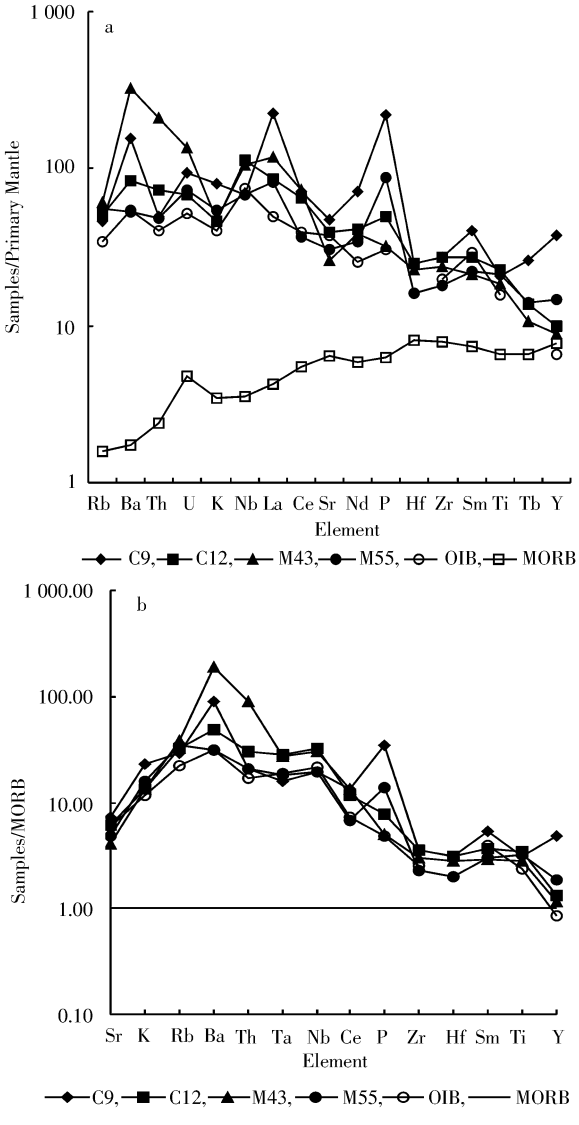


Fig. 5. Trace element spiderdiagram patterns of basalt samples. a. Primary mantle-normalized trace element spiderdiagram patterns of basalts. Normalized constants of primary mantle after McDonough et al. (1992), phosphorus constants after Sun (1980); and b. MORB-normalized trace element spiderdiagram patterns of basalts. Normalization constants of MORB after Saunders and Tarney (1984), OIB after Sun (1980).

salts is very different during secondary alteration. The active elements, such as uranium, potassium, rubidium, cesium, barium, and strontium, as well as volatile elements are very sensitive and can be easily leached due to secondary alteration (Pearce,

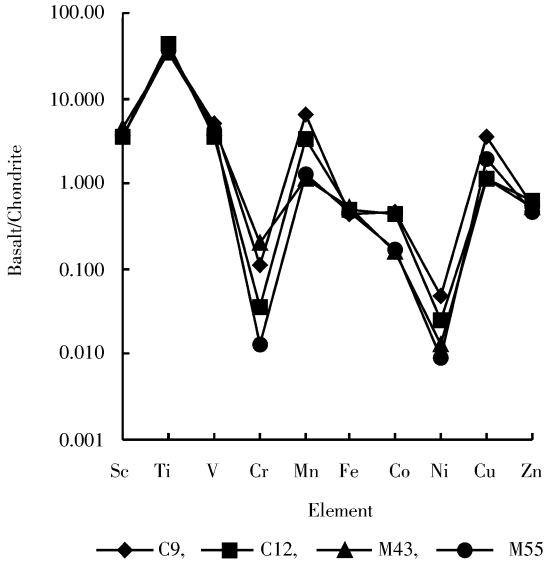


Fig. 6. Chondrite-normalized spiderdiagram patterns of transitional element for basalts. Normalized constants of chondrite after Langmuir et al. (1977), iron constants after Sun (1982).

1983). As a result, they are dispersed in the trace element spiderdiagram patterns (Fig. 5). The HFSE, such as titanium, zirconium, yttrium, niobium, tantalum, hafnium, and REE are relatively stable (Zhang, 1990) and not sensitive to post-petrogenetic alteration (Pearce, 1983). As a result, they record the initial features of basalts and usually have been used as indicators to identify the tectonic settings of the basalts (Pearce and Cann, 1973). The LREE are more active than the HREE, and are active in certain case, while HREE are too stable to change with secondary alteration (Condie, 1982).

The ratio of zirconium content to niobium one [$c$(Zr)/$c$(Nb)] is characteristically low in OIB (< 10) compared with N-type MORB (> 30) (Wilson, 1989). The ratios of $c$(Zr)/$c$(Nb) in basalt samples is in the range of 3.78 ~ 6.32 (see Table 2), having characteristics of OIB. The ratio $[c(\mathrm{La})/c(\mathrm{Sm})]_N$ (chondrite-normalized) of the samples is in the range of 3.18 ~ 5.67 (see Table 2), larger than 1, suggesting that the origin of ba-

salts is related to mantle plumes (Chen, 1990). Furthermore, the chondrite-normalized REE patterns (see Fig. 4) and trace element spiderdiagram patterns (see Fig. 5) of basalt samples are very similar to those of OIB, especially HREE and HFSE, indicating that the samples were initially typical intra plate OIB.

### 4.2 Basalt component change due to low-temperature alteration

During low-temperature reaction with seawater, basalts generally lose silicon, magnesium, calcium and $Fe^{2+}$ (MacGeehan and Maclean, 1980), and gain titanium, potassium, phosphorus, manganese, $iron_T$ and sodium (Hart, 1970). The major element contents of the basalt samples differ from those of basalts occurring in various geotectonic settings in the ocean and are depleted $SiO_2$, MgO, FeO and CaO but enriched $Fe_2O_3$, $K_2O$, MnO and $P_2O_5$ (see Table 1). Because of alteration, the major element contents of basalt samples deviate from their initial value and the samples lose the diagnostic characteristics of their primary rocks but record the information about secondary alteration.

The high contents of $Al_2O_3$, $H_2O$, $K_2O$ and REE of basalt samples were caused by leaching of magnesium, calcium, sodium, and $SiO_2$ to different degrees due to alteration and are therefore relatively enriched in the samples (Seyfried and Bischoff, 1979). The alteration of dark minerals, such as olivine, garnet, pyroxene, hornblende, magnetite and spinel, and of the matrix may be the primary reason for deviation of the major element contents. Because of alteration, the dark minerals were broken down. iron and magnesium therefore lost their host minerals and were intensively leached. As a result, they consumed less $SiO_2$ in the standard mineral calculation. Although $SiO_2$ was also depleted because of leaching, there is CIPW mineral quartz (Q). Compared with fresh OIB, the basalts have higher ratios of $c(Fe_2O_3)/c(FeO)$ and lower total iron contents $[c(Fe)]$ (see Table 1) which not only suggests that alteration is generally associated with an increase in oxidation state of iron (Pichler et al., 1999), but also that iron was leached from basalts as a result of alteration. It should be pointed out, that the higher MnO contents (in the range of 0.26% ~ 1.42%, with an average of 0.68%) of basalt samples than those of OIB and MORB (0.19% and 0.17%, respectively on the average) (see Table 1) were caused by precipitation of ferromanganese oxides in fissures and vesicles of the basalt (see Figs 2e and f).

Because REE are relatively stable in the supergene environment, there is no simple relationship between the activity of REE and rock types or degree of metamorphism. However, the mineral assemblage and fluid feature may be dominant factors in controlling the REE contents (Humphries, 1984). The similarity of REE patterns (see Fig. 4) between basalt samples and OIB (Hofmann and Jochum, 1996), as well as their higher REE contents than OIB (see Fig. 4) may suggest that the REE are more stable during low-temperature alteration and relatively enriched due to active elements leaching out from basalts. Furthermore, the precipitation of ferromanganese oxides which are relatively enriched in REE, especially LREE (see Table 2, Fig. 4), in fissures and vesicles of basalt (see Figs 2e and f), can cause not only the REE contents of basalt to increase but also the "fractionation" of their LREE and HREE. The samples therefore have high $\Sigma c(Ce)/\Sigma c(Yb)$ ratios (see Table 2 and Fig. 4).

### 4.3 Mass balance theoretical calculation

#### 4.3.1 *Calculation of total mass change caused by the alteration*

According to the above, REE can be relatively

enriched due to leaching of active components from basalts, and the precipitation of ferromanganese oxides (which have high contents of REE, especially LREE) in fissures and vesicles of altered basalts. In which, the latter can cause the REE contents to increase absolutely. REE are stable and are generally transported as a whole (Wang et al., 1989) so that their total contents can be used to calculate the mass balance. If we consider that the total change in the unit mass of fresh basalt is caused only by leaching of active components and by precipitation of ferromanganese oxides, the measured value of rare earth element $R$ can be given as follows:

$$R_M = (R_{OIB} + yR_{Fe-Mn})/(1 - x + y), \quad (1)$$

where $R_M$ is the measured value of rare earth element $R$, $R_{OIB}$ and $R_{Fe-Mn}$ are the contents of rare earth element $R$ of OIB and ferromanganese oxides, respectively; and $x$ and $y$ are the depleted quantities of unit mass of fresh basalt caused by alteration and the precipitated quantities of ferromanganese oxides in unit mass of fresh basalt, respectively. The expression $R_{OIB} + yR_{Fe-Mn}$ and $1 - x + y$ are therefore the quantity of rare earth element $R$ after alteration of unit mass of fresh basalt and the residual quantity for unit mass of fresh basalt after alteration, respectively.

Here we choose rare earth element neodymium and REE [$\Sigma c$(REE)] to substitute the quantity of rare earth element $R$, and from Eq. (1) we get:

$$c_M(Nd) = [c_{OIB}(Nd) + y \cdot c_{Fe-Mn}(Nd)]/(1 - x + y), \quad (2)$$

$$\Sigma c_M(REE) = [\Sigma c_{OIB}(REE) + y \cdot \Sigma c_{Fe-Mn}(REE)]/(1 - x + y), \quad (3)$$

where $c_M(Nd)$ and $\Sigma c_M(REE)$ are measured values of neodymium and the sum of REE content of basalt samples, respectively, $c_{OIB}(Nd)$ and $\Sigma c_{OIB}(REE)$ are neodymium content and the sum of REE content value of OIB, respectively, while $c_{Fe-Mn}(Nd)$ and $\Sigma c_{Fe-Mn}(REE)$ are neodymium content and the sum of REE content value of ferromanganese oxides, respectively. If we replace $y$ by $a$ and $1 - x + y$ by $b$, Eqs (2) and (3) can be simplified as follows:

$$c_M(Nd) = [c_{OIB}(Nd) + a \cdot c_{Fe-Mn}(Nd)]/b, \quad (4)$$

$$\Sigma c_M(REE) = [\Sigma c_{OIB}(REE) + a \cdot \Sigma c_{Fe-Mn}(REE)]/b. \quad (5)$$

From the set of Eqs (4) and (5), we can calculate $a$ and $b$ as follows:

$$a = [c_{OIB}(Nd) \cdot \Sigma c_M(REE) - c_M(Nd) \cdot \Sigma c_{OIB}(REE)]/[c_M(Nd) \cdot \Sigma c_{Fe-Mn}(REE) - c_{Fe-Mn}(Nd) \cdot \Sigma c_M(REE)]. \quad (6)$$

$$b = [c_{OIB}(Nd) \cdot \Sigma c_{Fe-Mn}(REE) - c_{Fe-Mn}(Nd) \cdot \Sigma c_{OIB}(REE)]/[c_M(Nd) \cdot \Sigma c_{Fe-Mn}(REE) - c_{Fe-Mn}(Nd) \cdot \Sigma c_M(REE)]. \quad (7)$$

If we choose $c_{OIB}$(Nd) $\Sigma c_{OIB}$(REE) of OIB as 30.87 μg/g and 140.30 μg/g (Hofmann and Jochum, 1996), respectively, and choose $c_{Fe-Mn}$(Nd) $\Sigma c_{Fe-Mn}$(REE) of Hawaii ferromanganese crusts as 371 μg/g and 3 485.17 μg/g (Hein et al., 1999), respectively (see Table 2), and substitute the contents and values of $c_{OIB}$(Nd) and $\Sigma c_{OIB}$(REE) of OIB, and $c_{Fe-Mn}$(Nd) and $\Sigma c_{Fe-Mn}$(REE) of Hawaii ferromanganese crusts into equation (6) and (7), we can derive $a$, $b$ and $x$, $y$. The results are listed in Table 3.

In Table 3, the depleted quantity for unit mass of fresh basalt caused by alteration is in the range of 0.150 ~ 0.657, and the precipitated quantity of ferromanganese oxides in unit mass of fresh basalt is 0.006 ~ 0.042. The residual quantity for unit mass of fresh basalt after alteration is therefore 0.353 ~ 0.892. In all the samples, Sample C9 is the one that has the largest depletion quantity (the depletion quantity for unit mass of fresh basalt is 0.657), which is consistent with its largest degree of alteration, while Sample M43 is the least altered but has largest amount of precipitated ferromanganese oxides (the ferromanganese oxides precipitated in unit mass of fresh basalt is 0.042) (see Table 3).

Table 3. Theoretical calculation results of total mass changes caused by the alteration

| Parameter | Explanation | C9 | C12 | M43 | M55 |
|---|---|---|---|---|---|
| $a$ | $y$ | 0.010 | 0.014 | 0.042 | 0.006 |
| $b$ | $1-x+y$, residual quantities for unit mass of fresh basalts | 0.353 | 0.643 | 0.892 | 0.700 |
| $x$ | depleted quantities for unit mass of fresh basalts | 0.657 | 0.371 | 0.150 | 0.306 |
| $y$ | precipitated quantities of ferromanganese oxides in unit mass of fresh basalts | 0.010 | 0.014 | 0.042 | 0.006 |

#### 4.3.2 *Calculation of the depleted quantities of metals and oxides for unit mass of fresh basalt*

Comparing with REE which are stable and not leached after petrogenesis, the active components can generally be leached from basalt to different degrees due to alteration. The changes in the quantity of metals and oxides of altered basalts are not only due to precipitation of ferromanganese oxides, but also to leaching of active components. If we consider the changes in quantities for fresh basalts due to alteration are caused only by precipitation of ferromanganese oxides in basalts, which "bring in" metals to the basalt, and by leaching of active components from basalts, which "take out" active components from basalt, the measured value of component $M$ can be expressed as follows:

$$c_{\mathrm{M}}(M) = [c_{\mathrm{OIB}}(M) + y \cdot c_{\mathrm{Fe-Mn}}(M) - c_{\mathrm{L}}(M)]/(1-x+y), \quad (8)$$

where $c_{\mathrm{M}}(M)$ is the measured value of component $M$ for basalt sample; $c_{\mathrm{OIB}}(M)$ and $c_{\mathrm{Fe-Mn}}(M)$ are contents of component $M$ for OIB and ferromanganese oxides, respectively; and $c_{\mathrm{L}}(M)$ is the depleted quantity of component $M$ for unit mass of fresh basalt due to alteration. The expression $c_{\mathrm{OIB}}(M) + y \cdot c_{\mathrm{Fe-Mn}}(M) - c_{\mathrm{L}}(M)$ is therefore the quantity of component $M$ for unit mass of fresh basalt after alteration, while $y$ and $1-x+y$ are the same means as above.

If we replace $y$ by $a$ and replace $1-x+y$ by $b$, Eq. (8) can be simplified as follows:

$$c_{\mathrm{M}}(M) = [c_{\mathrm{OIB}}(M) + a \cdot c_{\mathrm{Fe-Mn}}(M) - c_{\mathrm{L}}(M)]/b. \quad (9)$$

From Eq. (9), we can get $c_{\mathrm{L}}(M)$ as follows:

$$c_{\mathrm{L}}(M) = c_{\mathrm{OIB}}(M) + a \cdot c_{\mathrm{Fe-Mn}}(M) - b \cdot c_{\mathrm{M}}(M). \quad (10)$$

The values of the content of component $M$ for OIB $[c_{\mathrm{OIB}}(M)]$ and the content of component $M$ for ferromanganese crust $[c_{\mathrm{Fe-Mn}}(M)]$ are given in Tables 1 and 2 (the content of component $M$ for OIB $[c_{\mathrm{OIB}}(M)]$ is taken from Clague et al. (1980) and the content of component $M$ for ferromanganese crust $[c_{\mathrm{Fe-Mn}}(M)]$ from Hawaii is taken from Hein et al. (1999). By substituting the metal and oxide contents of OIB and ferromanganese oxides in Tables 1 and 2, and the values of $a$ and $b$ (listed in Table 3) into Eq. (10), we can derive the depleted quantity of metals or oxides for unit mass of fresh basalt caused by alteration. In Eq. (10), the expression $a \cdot c_{\mathrm{Fe-Mn}}(M)$ is the precipitated quantity of metals or oxides brought into unit mass of fresh basalt by ferromanganese oxides.

Table 4 lists the precipitated quantity of metals and oxides brought into unit mass of fresh basalt by ferromanganese oxides, the depleted quantities of metals and oxides from unit mass of fresh basalt, and the residual quantities of metals and oxides for unit mass of fresh basalt, as well as the depleted ratios (%) of metals and oxides for fresh basalts.

Table 4. The budget of transition metals and major oxides for unit mass of basalt due to alteration

| | Precipitated quantities of metals and oxides for unit mass of fresh basalt by precipitation of ferromanganese oxides | | | | Depleted quantities of metals and oxides for unit mass of fresh basalt | | | | Residualquantities of metals and oxides for unit mass of fresh basalt | | | | Depleted ratios (%) of metals and oxides for fresh basalt | | | |
|---|---|---|---|---|---|---|---|---|---|---|---|---|---|---|---|---|
| | $y \cdot c_{Fe-Mn}(M)$ | | | | $c_L(M)$ | | | | $c_{OIB}(M) + y \cdot c_{Fe-Mn}(M) - c_L(M)$ | | | | $c_L(M)/c_{OIB}(M)$ | | | |
| Element[1)] | C9 | C12 | M43 | M55 | C9 | C12 | M43 | M55 | C9 | C12 | M43 | M55 | C9 | C12 | M43 | M55 |
| Sc | 0.05 | 0.07 | 0.21 | 0.03 | 26.23 | 20.08 | 9.89 | 19.11 | 7.22 | 13.38 | 23.70 | 14.31 | 78.54 | 60.14 | 29.63 | 57.24 |
| Ti | 0.01 | 0.02 | 0.06 | 0.01 | 0.81 | 0.14 | 0.14 | 0.27 | 0.93 | 2.06 | 2.11 | 1.81 | 59.86 | 10.02 | 10.14 | 19.99 |
| V | 6.36 | 8.74 | 26.22 | 3.64 | 251.45 | 224.37 | 156.52 | 189.17 | 85.26 | 114.73 | 200.06 | 144.82 | 76.11 | 67.92 | 47.38 | 57.26 |
| Cr | 1.20 | 1.65 | 4.94 | 0.69 | 464.73 | 500.36 | 133.03 | 532.35 | 88.79 | 53.60 | 424.23 | 20.66 | 84.14 | 90.59 | 24.09 | 96.38 |
| Mn | 0.21 | 0.29 | 0.88 | 0.12 | −0.07 | 0.01 | 0.83 | 0.10 | 0.43 | 0.43 | 0.20 | 0.17 | −47.06 | 4.18 | 564.31 | 66.70 |
| Fe | 0.18 | 0.25 | 0.75 | 0.10 | 6.81 | 3.64 | 1.76 | 3.37 | 2.97 | 6.21 | 8.59 | 6.33 | 70.95 | 37.92 | 18.28 | 35.11 |
| Co | 70.10 | 96.40 | 289.20 | 40.10 | 55.96 | 26.59 | 284.90 | 48.42 | 77.68 | 133.35 | 67.84 | 55.22 | 88.06 | 41.84 | 448.37 | 76.20 |
| Ni | 37.07 | 50.98 | 152.93 | 21.21 | 118.67 | 142.07 | 286.43 | 203.80 | 162.86 | 153.37 | 110.97 | 61.87 | 48.54 | 58.12 | 117.17 | 83.37 |
| Cu | 7.72 | 10.61 | 31.83 | 4.41 | −35.73 | 20.44 | 14.20 | −55.23 | 139.81 | 86.53 | 113.99 | 156.01 | −37.08 | 21.22 | 14.74 | −57.32 |
| Zn | 5.39 | 7.41 | 22.24 | 3.08 | 26.21 | −41.73 | −58.33 | −22.45 | 67.36 | 137.32 | 168.75 | 113.72 | 29.73 | −47.32 | −66.15 | −25.46 |
| $SiO_2$ | 0.14 | 0.19 | 0.56 | 0.08 | 30.66 | 16.17 | 6.76 | 14.78 | 16.00 | 30.55 | 40.33 | 31.82 | 65.90 | 34.75 | 14.53 | 31.77 |
| $Al_2O_3$ | 0.03 | 0.04 | 0.13 | 0.02 | 8.84 | 2.39 | −3.06 | −1.65 | 5.72 | 12.18 | 17.72 | 16.20 | 60.87 | 16.46 | −21.07 | −11.36 |
| MgO | 0.02 | 0.03 | 0.09 | 0.01 | 8.76 | 5.84 | 4.15 | 7.60 | 0.59 | 3.51 | 5.26 | 1.73 | 93.94 | 62.62 | 44.50 | 81.52 |
| CaO | 0.03 | 0.05 | 0.14 | 0.02 | 6.69 | 6.94 | 2.36 | 5.55 | 3.69 | 3.45 | 8.11 | 4.81 | 64.68 | 67.13 | 22.87 | 53.68 |
| $Na_2O$ | 0.02 | 0.03 | 0.10 | 0.01 | 1.72 | 1.24 | 1.51 | 0.89 | 1.08 | 1.57 | 1.36 | 1.91 | 61.92 | 44.70 | 54.40 | 31.86 |
| $K_2O$ | 0.01 | 0.01 | 0.03 | 0.00 | 0.02 | −0.01 | −0.34 | −0.26 | 0.87 | 0.90 | 1.26 | 1.14 | 1.92 | −1.53 | −39.11 | −29.37 |
| $P_2O_5$ | 0.01 | 0.01 | 0.04 | 0.01 | −1.39 | −0.39 | −0.28 | −1.02 | 1.69 | 0.70 | 0.61 | 1.32 | −479.77 | −134.96 | −97.46 | −351.97 |

Notes: 1) The content unit of Sc, V, Cr, Co, Ni, Cu and Zn is microgram per gram; other unit is percentage.

### 4.3.3 *Estimate for the results of theoretical calculation*

In Fig. 4, the REE pattern positions of the four basalt samples have a sequence from low to high of Samples M43, C12, M55 and C9. This is quite similar to the theoretical calculation results listed in Table 3 (the bulk depleted quantities of the four samples for unit mass of fresh basalts are 0.150, 0.371, 0.306 and 0.657, respectively). REE are quite stable during alteration and their partition curve position in REE patterns is the result of leaching of active components from basalts and the precipitation of ferromanganese oxides in basalts. That is, the position deviation of their partition curve from that of fresh OIB in REE patterns indicates the alteration degree of basalts. With increasing alteration of the basalts, the more active components were leached out resulting in higher REE contents and higher $\Sigma c$(REE) values (see Fig. 7a), as well as the higher position on the REE partition curve (see Fig. 4) and vice versa. The ratio of $\Sigma c(Ce)/\Sigma c(Yb)$ is an important parameter indicating the degree of fractionation of the LREE and HREE, the higher ratios of $\Sigma c(Ce)/\Sigma c(Yb)$ reflecting the more intensive of the fractionation between LREE and HREE. In Table 2, Sample M43 shows the most intensive fractionation of LREE and HREE, with the $\Sigma c(Ce)/$

$\Sigma c$(Yb) ratio of 12.1, similar to that (14.89) of ferromanganese crusts (Hein et al., 1999). Sample C12 [with the $\Sigma c$(Ce)/$\Sigma c$(Yb) ratio of 8.73] and Sample C9 [with the $\Sigma c$(Ce)/$\Sigma c$(Yb) ratio of 7.16] occupy an intermediate position and Sample M55 is the one with the weakest fractionation of LREE and HREE with the $\Sigma c$(Ce)/$\Sigma c$(Yb) ratio of 6.0, which is much similar to that (5.39) of OIB (Hofmann and Jochum, 1996). There is a positive correlation between the ratios of $\Sigma c$(Ce)/$\Sigma c$(Yb) which reflect the degree of fractionation of LREE and HREE and the precipitation quantities of ferromanganese oxides in the basalts (Fig. 7b). The more ferromanganese oxides are precipitated in altered basalts, the higher are the ratio of $\Sigma c$(Ce)/$\Sigma c$(Yb) reflecting the more intensive fractionation of LREE and HREE (Fig. 7b), and vice versa. The leaching of active components from basalt can therefore cause the REE contents to increase and appears as translating the partition curves of REE patterns upwards; while the precipitation of ferromanganese oxides in basalts not only increases the REE contents and causes translation of partition curves of the REE patterns upwards but also increases the degree of "fractionation" of the LREE and HREE which induces an increase of curve slope in the REE patterns (see Fig. 4).

Of all the samples, Sample C9 has the largest depletion of active components (the depleted quantity for unit mass of fresh basalt is 0.657) and greatest degree of alteration, consistent with the largest negative cerium anomaly [$\delta$Ce = 0.45 (calculated by chondrite-normalized values, normalization constants of chondrite after Taylor and Mclennan, 1985)], which suggests that the cerium in the basalts was leached into seawater during low-temperature alteration. The weak negative cerium anomaly of Samples C12 and M43 (with $\delta$Ce values of 0.94 and 0.84, respectively) (see Table 2) are consistent with their high contents of ferromanganese oxides (with precipitated quantities of ferromanganese oxides in unit mass of fresh basalts of 0.014 and

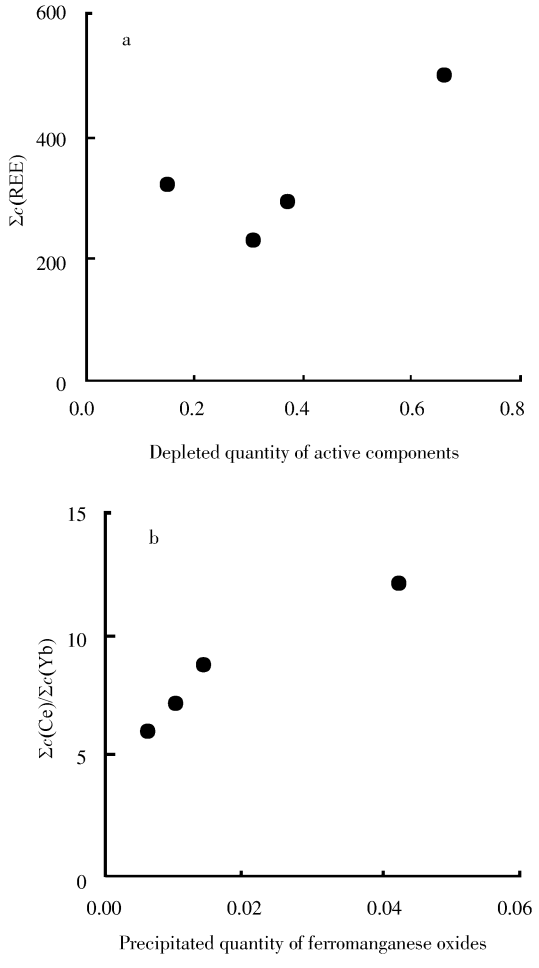


Fig. 7. Variation of REE parameters with leaching of active components and precipitation of ferromanganese oxides. a. Variation of $\Sigma c$(REE) with depleted quantity of active components. There is positive correlation between $\Sigma c$(REE) and depleted quantity of active components, the more active components leached, the bigger the $\Sigma c$(REE) values, indicating that leaching of active components results in an increase in $\Sigma c$(REE) values. b. Variation of the ratios of $\Sigma c$(Ce)/$\Sigma c$(Yb) with precipitated quantity of ferromanganese oxides. There is positive correlation between the ratios of $\Sigma c$(Ce)/$\Sigma c$(Yb) and ferromanganese oxides and precipitation of ferromanganese oxides in basalts which results in an increase of the ratios of $\Sigma c$(Ce)/$\Sigma c$(Yb) and an increase in the degree of fractionation between the LREE and HREE.

0.042, respectively) (see Table 3) implying that the precipitation of cerium-rich ferromanganese oxides in basalt flattened the negative cerium anomaly caused by alteration. Pichler et al. (1999) also suggested that the fractionation of $Ce^{4+}$ from the trivalent REE of altered basalts is largely due to selective adsorption of $Ce^{4+}$ by ferromanganese oxyhydroxides. In considering the negative cerium anomaly of altered basalts, the effect caused by the degree of alteration of the basalt and the effect caused by precipitation of ferromanganese oxides in basalts counteract each other. The negative cerium anomaly increases with the degree of alteration of the basalts, but can be flattened by precipitation of ferromanganese oxides in the basalts.

According to theoretical calculations, MgO has the largest depleted ratios (44.50% ~ 93.94%), and iron takes the second place (18.28% ~ 70.95%) (see Table 4). The depleted ratios of both MgO and iron exceed those of bulk rocks (15.0% ~ 65.7%) (see Table 3). The appearance of ferromanganese oxides and ferromanganese micronodules in altered basalts, and the lower iron contents of altered basalts (with the average of 9.19%) than those of fresh OIB (9.60%) (Clague et al., 1980), indicate that the amount of iron leached out from the basalts (with 1.76% ~ 6.81% of iron leached from unit mass of fresh basalt) is much more than that precipitated in basalts as ferromanganese oxides (with 0.10% ~ 0.75% of Fe brought in unit mass of fresh basalt by precipitated of ferromanganese oxides) (see Table 4). $SiO_2$ has the theoretical calculation depletion ratios of 14.53% ~ 65.90% (see Table 4), which is consistent with the bulk rock weight changes of 15.0% ~ 65.7% (see Table 3). Because of its depletion ratios are less than those of iron and magnesium (see Table 4), $SiO_2$ relatively enriched as a result of silicon supersaturation and quartz appears in the standard mineral calculation (see Table 1).

In Table 4, the depleted quantities of $P_2O_5$ from basalts for all the samples are "negative", indicating that the altered basalts is a "sink" rather than a "source" for phosphorus and that $P_2O_5$ was either not leached from the basalts during low-temperature or that the leached quantities of $P_2O_5$ are less than those precipitated in basalts by phosphatization. For some samples, the leached quantities of $Al_2O_3$, $K_2O$ are also negative, which may be related to the filling up of aluminium- and potassium-rich minerals, such as zeolite, in vesicle of basalts (see Fig. 2d). In Table 4, the elements, such as manganese, cobalt, nickel, copper, zinc, with very low contents in basalts but very high contents in ferromanganese oxides, sometimes have negative precipitation quantities or have precipitation quantities even exceed than 100% according to theoretical calculation. On one hand, it can easily cause error in theoretical calculations due to their very lower contents of these elements of basalt than those of ferromanganese oxides; on the other hand, it may indicate that these elements were not leached from basalts during low-temperature alteration but precipitated in basalts as ferromanganese oxides.

### 4.4 The contribution of low-temperature alteration of OIB to transition metal circulation of the ocean

In Table 4, the quantities of almost all the transition metal and other oxides introduced into basalts by precipitation of ferromanganese oxides are much lower than those leached out from basalts due to alteration. According to theoretical calculations, most elements were leached from basalts into seawater as a result of low-temperature alteration, while the others such as manganese, copper, and zinc sometimes precipitated into basalts from seawater as ferromanganese oxides and, in the case of aluminium and potassium, deposited in the vesicles of basalts as zeolite. Corresponding to fresh basalt, iron that is

1.76% ~ 6.81% of the fresh basalt is leached into seawater, while the quantities of iron precipitated as ferromanganese oxides is 0.10% ~ 0.75% of the fresh basalts. Therefore, the residual amount of iron is just 2.79% ~ 7.85% relative to fresh basalt [the contents of iron in fresh OIB is 9.60% on the average (Clague et al., 1980)] and more than 70% of iron of fresh basalt has been leached into seawater (see Table 4).

The volcanic rocks erupted in constructive plate boundaries are as much as 3 $km^3/a$, while the volcanic rocks erupted in oceanic intra plate are less than an order of magnitude, with about 0.3 ~ 0.4 $km^3/a$ (McBirney, 1984). The formation of oceanic crusts is much faster than that of volcanic rocks, with a rate of 15 $km^3/a$ (Williams and von Herzen, 1974) and a mass of 50 Gt (Seyfried and Mottl, 1982). If we assume that about 5% of OIB were altered, there would be 3 Gt of manganese and 200 Gt of iron leached into seawater per Ma, other trace transition metals leached into seawater would generally be 100 ~ 500 Mt/Ma. Which can satisfy the requirement of metals for the formation of 5 mm thick of cobalt-rich ferromanganese crusts at least $1 \times 10^6$ ~ $2 \times 10^7 km^2/Ma$. OIB is an important metal source of the ocean.

Cobalt-rich ferromanganese crusts are formed by hydrogenetic precipitation (Hein et al., 1999) with the elements precipitated directly from seawater (Koschinsky and Halbach, 1995; Seibold and Berger, 1993; Halbach et al., 1981). The ultimate sources of metals to the oceans are river and eolian input, hydrothermal input, weathering of basalts, release of metals from sediments, and extraterrestrial input (Hein et al., 1999). Cobalt-rich ferromanganese crusts are ubiquitous on hard-rock substrate of submarine highs (Glasby, 2006; Aplin and Cronan, 1985; Hein et al., 1985). They form on the flanks and summits of seamounts, ridges, plateaus, and abyssal hills where the rocks have been swept clean of sediments (von Blanckenburg et al., 1996; Halbach and Puteanus, 1984). The sweep of sediments from abyssal hills keeps the outcrops of basalts exposed to seawater which not only induces to the formation of cobalt-rich crusts but also facilitates the low-temperature alteration of basement basalts. When ocean islands were sinking to form submarine seamounts, iron, manganese and other transition metals were leached out from basalts due to low-temperature alteration, which supplied ore-forming metals to cobalt-rich crusts. Because of its high affinity with oxygen (Liu, 1984), iron leached into seawater from basalts can easily precipitate in situ. If this is correct, the occurrence of cobalt-rich ferromanganese crusts on the outcrops of basalts may be an important indicator for weathering of basalts, and cobalt-rich ferromanganese crusts could be regarded as a so called "crust of weathering" to identify the degree of weathering of the basalt.

The decomposition of the dark minerals, as well as precipitation of ferromanganese oxides in fissures and vesicles of basalts indicate that the basalt samples were altered. This led to leaching of iron, manganese and other transition metals into seawater and implies that oceanic basalts are an important source of metals in the formation of ferromanganese crusts. The fact of most ferromanganese crusts distributed on submarine seamounts, as well as those have thick crusts and with high economic values generally precipitated on the surface of intensively altered basalts (Hein and Morgan, 1999; De Carlo et al., 1987) or on the surface of oceanic basalts (Koschinsky et al., 1997) suggests that the formation of ferromanganese crusts is related to low-temperature alteration of oceanic basalts and that the seafloor basalts may be an important ore-forming source for ferromanganese crusts. The precipitation of ferromanganese micronodules (see Fig. 2e) and ferromanganese oxides (see Fig. 2f) in vesicles and fissures of altered basalts may offer the best evidence that iron, manga-

nese and other transition metals of ferromanganese crusts may be derived primarily from low-temperature alteration of basalts. This is consistent with strontium, neodymium, and lead isotope studies of ferromanganese crusts and basalts (O'Nions et al., 1978).

The increase in the ratio of $c(Fe_2O_3)/c(FeO)$ and $H_2O$ and $K_2O$ contents and the decrease of MgO contents resulted from alteration of basalts (Hekinian, 1971). The further from the axes of mid-ocean ridges, the older the oceanic basin basalts, and the more intensively altered are the seafloor basalts (Thompson, 1983). However, the thickness of sediments covered on oceanic basin will increase with the increase of oceanic crust ages (Banakar et al., 1997). Once the oceanic basin basalts (MORB) were covered by impermeable clayey sediments, the halmyrolysis of basalts would decrease significantly (Chamley, 1989). Submarine seamounts are cliffy and the basement basalt (OIB) is mostly exposed as outcrop, which makes continuous alteration of OIB possible. The altered seafloor basalt (MORB) has the ratio of $c(Fe_2O_3)/c(FeO)$ less than 2.2, and $H_2O$ contents less than 5.2% (Hekinian, 1971) while the altered OIB has the ratio of $c(Fe_2O_3)/c(FeO)$ greater than 10 and LOI contents greater than 10% (see Table 1). Higher $c(Fe_2O_3)/c(FeO)$ ratios of samples suggest more intensive alteration of the basalts (Qiu, 1991). If we use the ratio of $c(Fe_2O_3)/c(FeO)$ and $H_2O$ contents as indices to evaluate the intensity of alteration of basalt, OIB exposed as outcrops are altered more intensively than seafloor basalt (MORB) which is covered by sediment soon after their migration from the mid-ocean ridge. Although the eruption rate of OIB is limited (0.3 ~ 0.4 $km^3/a$) (McBirney, 1984), they were altered intensively. The eruption rate of seafloor basalts (MORB) is higher (3 $km^3/a$) (McBirney, 1984) but their permeability decreases due to covering by sediment soon after their migration-from the mid-ocean ridge. As a result, alteration of seafloor basalts is limited.

## 5 Conclusions and summary

Altered basalts from the central and western Pacific ferromanganese crust province have REE and trace elements characteristics of oceanic intra plate basalts derived from OIB.

The alteration of basalts causes their $Al_2O_3$, $Fe_2O_3$, MnO, $K_2O$, and $P_2O_5$ contents to increase and MgO, FeO contents to decrease. The increase in the REE contents of basalts resulted from leaching of the active components during alteration while precipitation of the LREE-rich ferromanganese oxides in fissures and vesicles of basalts not only introduced REE into the basalts but also resulted in "fractionation" of the REE in the altered basalts due to the precipitation of LREE-rich ferromanganese oxides in the basalts. The leaching of active elements from the basalts and precipitation of authogenic components in the basalts are the two most important mechanisms causing the composition of samples to deviate from that of fresh basalts.

Theoretical calculations indicate that the residual quantity for unit mass of fresh basalts is in the range of 0.353 ~ 0.892. Of the all the elements, Magnesium has the largest leaching ratios (44.50% ~ 93.94%) and iron takes the second place (18.28% ~ 70.95%). The leached ratios of both magnesium and iron exceed the decrease of bulk rocks (15.0% ~ 65.7%). $SiO_2$ has the theoretical calculation leaching ratios of 14.53% ~ 65.90% similar to that of bulk rocks (15.0% ~ 65.7%). The negative depletion quantities of aluminium, potassium, and phosphorus in some samples results from the occupancy of these elements in aluminium- and potassium-rich minerals, such as zeolite, in vesicles of the basalt or from phosphatisation of the basalts.

OIB may be an important "source" for transition metal circulation in seawater, while ferromanganese crusts and ploymetallic nodules may be important "sink". The transition metals leached from OIB into seawater can satisfy the requirement of the formation of 5 mm thick layer of ferromanganese deposits covering an area of $1 \times 10^6 \sim 20 \times 10^6$ km$^2$/Ma. Low-temperature alteration of oceanic basalts may therefore represent an important source of transition metals for formation of ferromanganese oxides.

## *Acknowledgements*

Dr. Glasby G P is thanked for his careful review of this paper. We would like to thank the crews on R. V. *Dayang* No. 1 in 1999 for dredging the ferromanganese crusts investigated in this study and to thank the referees for their helpful advice.

## References

Aplin A C, Cronan D S. 1985. Ferromanganese oxide deposits from the Central Pacific Ocean: I. Encrustations from the Line Island Archipelago. Geochim Cosmochim Acta, 49: 427 ~ 436

Banakar V K, Pattan J N, Mudholkar A V. 1997. Palaeoceanographic conditions during the formation of a ferromanganese crust from the Afanasiy—Nikitin seamount, North Central Indian Ocean: geochemical evidence. Mar Geol, 136: 299 ~ 315

Chamley H. 1989. Clay Sedimentology. Berlin: Springer, 291 ~ 329

Chen Deqian. 1990. Practical Rare Earth Element Geochemistry (in Chinese). Beijing: Metallurgical Industry Press, 59 ~ 114

Chester R. 2000. Marine Geochemistry. 2nd ed. Oxford: Blackwell Science, 88 ~ 97

Clague D A, Jackson E D, Wright T L. 1980. Petrology of Hualalai volcano, Hawaii: implication for mantle composition. Bull Volcano, 43: 641 ~ 656

Condie K C. 1982. Plate Teconic and Crustal Evolution. New York: Pergamon Press, 258

Dang Zhi, Hou Ying. 1995. Experimantal Study on the Dissolution Kinetics of Basalt water Interaction. Acta Petrologica Sinica (in Chinese), 11: 9 ~ 15

De Carlo E H, McMurtry G M, Kim K H. 1987. Geochemistry of ferromanganese crusts from the Hawaiian Archipelago: I. Northern survey areas. Deep-Sea Research, 34: 441 ~ 467

Furnes H, Staudigel H. 1999. Biological mediation in ocean crust alteration: how deep is the deep biosphere? Earth Planet Sci Lett, 166: 97 ~ 103

Glasby G P. 2006. Manganese: Predominant role of nodules and crusts. In: Schulz H D, Zabel M, eds. Marine Geochemistry, 2nd ed. Heidelberg: Springer, 371 ~ 427

Halbach P, Hebisch U, Scherhag C. 1981. Geochemical variations of ferromanganese nodules and crusts from different provinces of the Pacific Ocean and their genetic control. Chem Geol, 34: 3 ~ 17

Halbach P, Puteanus D. 1984. The influence of the carbonate dissolution rate on the growth and composition of Co-rich ferromanganese crusts from Central Pacific seamount areas. Earth Planet Sci Lett, 68: 73 ~ 87

Hart R. 1970. Chemical exchange between sea water and deep ocean basalts. Earth Planet Sci Lett, 9(3): 269 ~ 279

Hein J R, Koschinsky A, Bau M, et al. 1999. Cobalt-rich ferromanganese crusts in the Pacific. In: Cronan D S, eds. Handbook of Marine Mineral Deposits. Boca Raton: CRC Press, 239 ~ 279

Hein J R, Manheim F T, Schwab W C, et al. 1985. Ferromanganese crusts from Necker ridge, Horizon Guyot and S. P. Lee Guyot: geological considerations. Mar Geol, 69: 25 ~ 54

Hein J R, Morgan C L. 1999. Influence of substrate rocks on Ferromanganese crust composition. Deep-Sea Research, 46: 855 ~ 875

Hekinian R. 1971. Chemical and mineralogical differences between abyssal hill basalts and ridge tholeiites in the Eastern Pacific Ocean. Mar Geol, 11: 77 ~ 91

Hofmann A W, Jochum K P. 1996. Source characteristics derived from very incompatible trace elements in Mauna Loa and Mauna Kea basalts, Hawaii Scientific Drilling Project. Geophys Res, B101: 11831 – 11839

Honnorez J. 1981. The aging of the oceanic crust at low temperature. In: Emiliani C, ed. The Sea, v 7: The Oceanic

Lithosphere. New York: Wiley & Sons, 525 ~ 587

Humphries S E. 1984. The mobility of the rare earth elements in the crust. In: Henderson P, ed. Rare Earth Element Geochemistry. Amsterdam: Elsevier, 315 ~ 341

Kang Xiangui, Kang Chansheng, Yang Rongyong. 1998. Research on the basalt nuclei of polymetallic nodules from the east Pacific Basin. Geological Journal of China Universities (in Chinese), 4: 147 ~ 154

Koschinsky A, Halbach P. 1995. Sequential leaching of marine ferromanganese precipitates: genetic implications. Geochim Cosmochim Acta, 59: 5113 ~ 5132

Koschinsky A, Stascheit A, Bau M, et al. 1997. Effects of phosphatization on the geochemical and mineralogical composition of marine ferromanganese crusts. Geochim Cosmochim Acta, 61: 4079 ~ 4094

Langmuir C H, Bender J F, Bence A E, et al. 1977. Petrogenesis of basalts from the FAMOUS area: mid-Atlantic ridge. Earth Planet Sci Lett, 36: 133 ~ 156

Le Maitre R W. 1989. A Classification of Igneous Rocks and Glossary of Terms. Oxford: Blackwell Scientific Publications, 193

Li Xuelun. 1997. Marine Geology (in Chinese). Qingdao: Press of Qingdao Ocean University, 179

Liu Yingjun. 1984. Element Geochemistry (in Chinese). Beijing: Science Press, 80 ~ 85

MacGeehan P J, Maclean W H, 1980. An Archaean sub-seafloor geothermal system, "calc-alkali" trends, and massive sulphide genesis. Nature, 286: 767 ~ 771

McBirney A R. 1984. Igneous Petrology. San Francisco: Freeman, Cooper, 504

McDonough W F, Sun S S, Ringwood A E, et al. 1992. K, Rb and Cs in the earth and moon and the evolution of the earth's mantle. Geochim Cosmochim Acta, 56: 1001 ~ 1012

Miyashiro A, Shido F, Ewing M. 1969. Diversity and origin of abyssal tholeiite from the Mid-Atlantic Ridge near 24° and 30° north latitude. Contrib Mineral Petrol, 23: 38 ~ 52

Moore J G. 1966. Rate of palagonitization of submarine basalt adjacent to Hawaii. U S Geol Surv Prof Pap, 550 – D, 163 ~ 171

Mottl M J, Holland H D. 1978. Chemical exchange during hydrothermal alteration of basalt by seawater: I. Experimental results for major and minor components of seawater. Goechim Cosmochimia Acta, 42: 1103 ~ 1115

Mukhopadhyay R, Iyer S D, Ghosh A K. 2002. The Indian Ocean nodule field: petrotectonic evolution and ferromanganese deposits. Earth Science Reviews, 60: 67 ~ 130

O'Nions R K, Carter S R, Cohen R S, et al. 1978. Pb, Nd and Sr isotope in oceanic ferromanganese deposits and ocean floor basalts. Nature, 273: 435 ~ 438

Pearce J A. 1983. Role of the sub-continental lithosphere in magmas genesis at active continental margins. In: Hawkesworth C J, Norry M J, eds. Continental Basalts and Mantle Xenoliths. Nantwich: Shiva, 230 ~ 249

Pearce J A, Cann J R. 1973. Tectonic setting of basalt volcanic rocks determined using trace element analysis. Earth Planet Sci Lett, 19: 290 ~ 300

Pichler T, Ridley W I, Nelson E. 1999. Low-temperature alteration of dredged volcanics from the Southern Chile Ridge: additional information about early stages of seafloor weathering. Mar Geol, 159: 155 ~ 177

Qi Liang, Grégoire D C. 2000. Determination of trace elements in twenty six Chinese geochemistry reference materials by Inductively Coupled Plasma – Mass Spectrometry. Geostandards Newletters, 24(1): 51 ~ 63

Qiu Jiaxiang. 1991. Applied Magmatic Petrology (in Chinese). Wuhan: Press of China Geology University, 155 ~ 224

Qiu Jiaxiang. 1985. Magmatic Petrology (in Chinese). Beijing: Geology Press, 190 ~ 206

Saunders A D, Tarney J. 1984. Geochemical characteritics of basaltic volcanism within back arc basins. In: Kokelaar B P, Howells M F, eds. Marginal Basin Geology, v 16, London: Spec Publ Geol Soc, 59 ~ 76

Schilling J G, Zajac M, Evans R, et al. 1983. Petrologic and geochemical variations along the Mid-Atlantic Ridge from 27°N to 73°N. Am Sci, 510 ~ 586

Seewaid J S, Seyfried W E Jr. 1990. The effect of temperature on metal mobility in subseafloor hydrothermal system: constraints from basalt alteration experiments. Earth Planet Sci Lett, 101: 388 ~ 403

Seibold E, Berger W H. 1993. The Sea Floor—An Introduction to Marine Geology. Berlin: Springer – Verlag, 289 ~ 294

Seyfried W E Jr, Bischoff J L. 1979. Low temperature basalt alteration by seawater: an experimental study at 70℃ and 150℃. Goechim Cosmochim Atca, 43: 1937 ~ 1947

Seyfried W E Jr, Mottl M J. 1982. Hydrothermal alteration of basalt by seawater under seawater dominated conditions. Goechim Cosmochim Atca, 46: 985 ~ 1002

Staudigel H, Hart S R. 1983. Alteration of basaltic glass: mechanisms and significance for the oceanic crust – seawater budget. Geochim Cosmochim Acta, 47: 337 ~ 350

Sun Shanshu. 1982. Chemical composition and origin of the earth's primitive mantle. Geochim Cosmochim Acta, 46: 179 ~ 192

Sun Shanshu. 1980. Lead isotopic study of young volcanic rocks from mid-ocean ridges, ocean islands and island arcs. Phil Trans R Soc Lond, A297, 409 ~ 445

Taylor S R, Mclennan S M. 1985. The Continental Crust: Its Composition and Evolution. Oxford: Blackwell Scientific Publication, 209 ~ 230

Thompson G. 1983. Hydrothermal Fluxes in the Ocean. In: Riley J P, Chester R, eds. Chemical Oceanography. New York: Academic Press, 271 ~ 337

Thompson G. 1991. Metamorphic and Hydrothermal Processes: Basalt Seawater Interactions. In: Floyd P A, ed. Oceanic Basalts. Glasgow: Blackie and Sons, 148 ~ 173

von Blankenburg F, O'Nions R K, Belshaw A, et al. 1996. Global distribution of beryllium isotopic in deep ocean water as derived from Ferromanganese crusts. Earth Planet Sci Lett, 141: 213 ~ 226

Wang Zhonggang, Yu Xueyuan, Zhao Zhenhua. 1989. Rare Earth Element Geology (in Chinese). Beijing: Science Press, 535

Williams D L, von Herzen R P. 1974. Heat loss from the earth: new estimate. Geology, 2: 327 ~ 328

Wilson M. 1989. Igneous Petrogenesis. London: Unwin Hyman, 245 ~ 285

Zhang Qi. 1990. The correct use of the basalt discrimination diagram. Acta Petrologica Sinica (in Chinese), 2: 87 ~ 94